1   **Title**

2   EXOCYST70A3 controls root system depth in Arabidopsis via the dynamic modulation of auxin

3   transport

4

5   **Authors**

6   Takehiko Ogura[1,2], Christian Goeschl[2], Daniele Filiault[2], Madalina Mirea[2], Radka Slovak[2†], Bonnie

7   Wolhrab[2], Santosh B. Satbhai[1,2‡], and Wolfgang Busch[1,2]*

8

9   **Affiliations**

10   [1] Plant Molecular and Cellular Biology Laboratory, and Integrative Biology Laboratory, Salk

11   Institute for Biological Studies, La Jolla, United States of America

12   [2] Gregor Mendel Institute (GMI), Austrian Academy of Sciences, Vienna Biocenter (VBC), Dr.

13   Bohr-Gasse 3, 1030 Vienna, Austria

14   [†] Present address: Department of Plant Sciences, University of Oxford, South Parks Road, Oxford

15   OX1 3RB, UK

16   [‡] Present address: Department of Biological Sciences, Indian Institute of Science Education and

17   Research (IISER) Mohali, Punjab, India

18

19   **Contact**

20   * Correspondence: wbusch@salk.edu

21   Phone: +1 858 453 4100 x1765

1   **SUMMARY**

2   Root system architecture (RSA), the distribution of roots in soil, plays a major role in plant survival.

3   RSA is shaped by multiple developmental processes that are largely governed by the

4   phytohormone auxin, suggesting that auxin regulates responses of roots that are important for

5   local adaptation. However, auxin has a central role in numerous processes and it is unclear which

6   molecular mechanisms contribute to the variation in RSA for environmental adaptation . Using

7   natural variation in *Arabidopsis*, we identify *EXOCYST70A3* as a modulator of the auxin system

8   that causes variation in RSA by acting on PIN4 protein distribution. Allelic variation and genetic

9   perturbation of *EXOCYST70A3* leads to alteration of root gravitropic responses, resulting in a

10 different RSA depth profile and drought resistance. Overall our findings suggest that the local

11 modulation of the pleiotropic auxin pathway can gives rise to distinct root system architectures

12 that can be adaptive in specific environments.

13 (150/150 words)

14

15 **INTRODUCTION**

16 The root system enables plants to anchor themselves in the soil and forage their environment for

17 nutrients and water. The evolution of this system 400 million years ago allowed plants to efficiently

18 colonize and transform the land surface of our planet (Algeo and Scheckler, 1998; Gibling and

19 Davies, 2012), paving the way for the highly diverse ecosystems that occupy its landmasses today.

20 The modern root system of dicot species, such as the model plant *Arabidopsis thaliana*, consists

1   of a single primary root that emerges from the seed coat, often remains active throughout the

2   plant's lifespan, and can develop several orders of lateral roots (Atkinson *et al.*, 2014; Peret *et al.*,

3   2009). The apical growth of each root in a root system is driven by cell divisions and subsequent

4   cell expansions in a stem-cell containing structure called the root apical meristem that is located in

5   each root tip (Benfey and Scheres, 2000). Depending on the direction of root growth, different

6   areas in the soil are explored (i.e. a downward growing root will explore the soil vertically and a

7   sideways growing root will explore it horizontally). The number and position of lateral roots add to

8   this complexity and determine which soil layers are intensively explored. All these processes

9   shape root system architecture (RSA) – the spatial distribution of the roots in the soil (Jung and

10   McCouch, 2013). RSA determines important physiological properties of a root system including

11   nutrient and water uptake and anchoring in the soil (Den Herder *et al.*, 2010). Despite the

12   importance of RSA, the genes and molecular mechanisms that govern RSA in natural

13   environments remain largely unknown nor do we fully understand which RSA types confer fitness

14   to a particular environment.

15   Various basic developmental processes that shape RSA including root elongation, gravitropism

16   and lateral root development are regulated by the phytohormone auxin (Pierik and Testerink,

17   2014). Therefore, it is most likely that auxin plays an important role in the variation in RSA in

18   different environments. However, auxin is a ubiquitous regulator of almost every aspect of plant

19   growth and development at the molecular, cellular, tissue, and organ levels (Benjamins and

20   Scheres, 2008; De Rybel *et al.*, 2009). It is therefore not clear which genetic and molecular

3

1   mechanisms modulate auxin signaling to give rise to the observed natural variation of RSA

2   without disrupting general auxin pathway.

3   Here, using natural variation and genome wide association mapping in *A. thaliana*, we identify a

4   gene, *EXOCYST70A3*, which regulates RSA by controlling the auxin pathway but independently

5   from other general auxin-dependent growth processes. *EXOCYST70A3* affects the distribution of

6   the PIN4 protein, suggesting that a PIN4-related auxin pathway can be specifically modulated by

7   a component of the exocytosis pathway. We show that allelic variation and genetic perturbation of

8   *EXOCYST70A3* lead to alterations in the orientation of root growth, resulting in a shift from

9   shallow to deep root systems. Finally, guided by data showing that the distribution of

10   *EXOCYST70A3* alleles is highly correlated with precipitation seasonality, a measure of rainfall

11   patterns, we show that overexpression and allelic variation of *EXOCYST70A3* affect drought

12   resistance and conclude that *EXOCYST70A3* variation may play an adaptive role in areas with

13   variable rainfall patterns.

14

15   **RESULTS**

16   ***EXOCYST70A3* is associated with natural variation of agravitropic root growth upon auxin**

17   **transport perturbation**

18   To identify components which regulate RSA related traits by the regulation of auxin pathway, we

19   capitalized on the extensive natural variation of root growth among natural accessions of the

20   model plant *A. thaliana* (Gifford *et al.*, 2013; Slovak *et al.*, 2014). In particular, we applied a

4

1   chemical genetics approach using the auxin transport inhibitor 1-*N*-naphtylphthalamic acid (NPA,

2   10 μM) and assessed the sensitivity of 215 *A. thaliana* natural accessions (Table S1) to

3   perturbation of auxin transport (Figure 1A). Notably, the response to NPA in terms of root growth

4   direction (horizontality, an index of root agravitropism which captures the extent of root growth in

5   the horizontal direction, see supplementary information for details of the trait), a key trait for RSA,

6   was highly variable among accessions in comparison to other traits including total length (Figure

7   1B, S1). Using genome wide association (GWA) mapping to identify loci underlying the variation

8   of horizontality upon NPA treatment, we detected a peak containing a highly significantly

9   associated Single Nucleotide Polymorphisms (SNP) on chromosome 5 (Figure 1C-D, Table S2).

10   This SNP showed considerable effect size (13.58%), suggesting a strong allele effect of the locus

11   which was tagged by this SNP. Using haplotype analysis of the 40 KB region centered on this SNP,

12   we classified the tested accessions into two haplogroups and observed that one haplogroup was

13   significantly associated with greater horizontality (population structure corrected association test:

14   *p*-value = 4.3×10^{-3}, Figure S2A), indicating that accessions in this haplogroup show increased

15   responses in root growth direction to NPA. Hereafter, this haplogroup is referred to as haplogroup

16   H (High-response to NPA, containing 16 accessions) and the other as haplogroup C

17   (Common-response to NPA, containing 199 accessions including Col-0).

18   Having identified a genomic region associated with control of root growth direction, we set out to

19   identify the causal gene (Table S2, Figure S2B). The significantly-associated SNP identified by

20   GWA mapping is located in the protein-coding region of the *EXOCYST70A3* gene (AT5G52350,

5

1   hereafter called *EXO70A3*). EXO70A3 is a homologue of yeast and Human EXO70, which is one

2   subunit of the octameric vesicle-tethering EXOCYST complex (Kee *et al.*, 1997; TerBush *et al.*,

3   1996). Human EXO70 directs vesicles to target locations on the plasma membrane (Matern *et al.*,

4   2001). The association of the root growth direction phenotype with variation in a central

5   component for exocytosis was striking, since its counterpart, endocytosis, is recognized as one of

6   main regulatory processes for localization of the PIN-FORMED (PIN) auxin efflux carriers and

7   therefore critical in regulating auxin signaling (Petrasek and Friml, 2009). Importantly, a

8   microarray based high-resolution root expression atlas (Brady *et al.*, 2007) showed that *EXO70A3*

9   transcripts are specifically expressed in the root tip and the elongation zone (Figure 2A, S3A-D),

10   which are the main sites for gravity perception and directional growth responses, respectively

11   (Masson *et al.*, 2002). In line with this, an independently generated RNA-Seq based atlas also

12   showed columella cell-specific expression of *EXO70A3* (Figure S3E, Li *et al.*, 2017). Consistent

13   with both these studies, we could only detect expression of *EXO70A3* in the root tip and not in

14   whole roots or shoots (Figure 2B). Taken together our data strongly suggested the involvement of

15   *EXO70A3* in the determination of root growth direction via an auxin pathway (designated ARD:

16   Auxin-dependent Root Directional growth), and led us to further analyze *EXO70A3* function.

17

18   **EXO70A3 alleles cause natural variation of responses to NPA in roots**

19   To characterize *EXO70A3,* we obtained a T-DNA line (SALK_075426; hereafter called

20   *EXO70A3ox*) which has a promoter insertion resulting in the strong overexpression of *EXO70A3*

6

1   (Figure 2A, B) but not of the surrounding genes (Figure. S3F, G). In addition, we generated

2   another overexpression line that ubiquitously highly expresses *EXO70A3* using a *35S* promoter

3   (*35S::GFP:EXO70A3*), and two *CRISPR/CAS9*-based knockout lines (*CRISPR-exo70A3-1* and

4   *CRISPR-exo70A3-2*) each containing an early stop codon (Figure 2A, B). The effect of NPA on

5   the direction of root growth of these four mutants was tested on MS medium supplemented with a

6   low dose of NPA (0.5 μM) or control medium. The direction of root growth on medium containing

7   NPA was significantly more agravitropic in the four mutant lines of *EXO70A3* (two-way ANOVA,

8   genotype-treatment interaction *p*-value < 0.05, Figure 3A), suggesting that ARD is misregulated in

9   both, knockout and overexpression lines of *EXO70A3* due to the loss of the appropriate

10   spatio-temporal expression pattern of *EXO70A3*. We then tested whether *EXO70A3* itself is auxin

11   regulated, but neither IAA nor NPA up/downregulated *EXO70A3* expression levels in Col-0 (Figure

12   2C), indicating that *EXO70A3* function itself is auxin-independent.

13   Next, we tested the causality of alleles that we had identified in our GWAS by allelic

14   complementation analysis. We therefore fused *EXO70A3* promoter sequence from Col-0 to the

15   protein coding region of *EXO70A3* of five natural accessions (Haplogroup C: Col-0, Shakdara

16   (Sha), Lp2-2. Haplogroup H: LAC-5, Coc-1. Figure S2C) and transformed these constructs into

17   the *CRISPR-exo70A3-1* line. We reasoned that if the *EXO70A3* alleles of the two haplogroups

18   were underlying the observed phenotypes, they should complement the knockout mutant

19   phenotype to a different extent.

20   While we could not observe any complementation of the knockout mutant phenotype with an

1   empty vector control, we achieved full complementation with the Col-0 allele belonging to

2   haplogroup C (ANOVA: p-value < 0.05, Post hoc Tukey test: *p*-value < 0.05, Figure 3B). In

3   contrast to the C haplogroup Col-0 *EXO70A3* allele, all complementations with haplogroup H

4   alleles (Lac-5, Coc-1) resulted in similar phenotypes with *EXO70A3* mutants and a natural

5   accession from haplogroup C, Coc-1 (Figure S2D), and did not lead to a significant

6   complementation of the NPA-induced root growth direction phenotype (Figure 3B).

7   Complemention with further haplogroup C accession alleles (Sha, Lp2-2) were in between the

8   Col-0 complementation and the haplogroup H non-complementation (Figure 3B). Consequently,

9   when testing whether haplogroup H and haplogroup C were different in their ability to complement,

10 the 2-way ANOVA resulted in a high significance (haplogroup - treatment interaction *p*-value =

11 9.36×10^{-7}), demonstrating that allelic variation of *EXO70A3* determines natural variation of ARD.

12 Since the two constructs that were created with *EXO70A3* sequences from haplogroup H

13 contained single non-synonymous SNP which exists only in haplogroup H in our analysis

14 (Chromosome 5, 21257230, Figure S2C), this coding change is the prime candidate for conferring

15 this effect.

16

17 ***EXO70A3* specifically regulates gravitropic responses of PIN4 in columella cells**

18 Since allelic variation of *EXO70A3* was causal for the natural variation of the root response to NPA,

19 we set out to investigate the mechanism for the involvement of *EXO70A3* in the regulation of

20 auxin signaling. We first assessed the effects of *EXO70A3* on the localization patterns of the PIN

1   auxin efflux carriers by crossing *EXO70A3ox* with widely used *PIN::PIN:GFP* plants. Of the eight

2   members of the Arabidopsis PIN family, five PINs (PIN1, PIN2, PIN3, PIN4 and PIN7) that are

3   widely recognized for their fuctions in roots were tested. While PIN1, PIN2, PIN3, and PIN7

4   localization were not substantially affected (Figure S4A), PIN4:GFP was superabundant in

5   columella cells of primary roots but not in stele cells in *EXO70A3ox PIN4::PIN4:GFP* plants

6   (Figure 4A, B). In these plants, almost all cells in the columella tissue showed PIN4:GFP signal

7   while only a fraction of cells in the columella tissue showed signal in the control *PIN4::PIN4:GFP*

8   plants. In both *PIN4::PIN4:GFP* and *EXO70A3ox PIN4::PIN4:GFP* plants, PIN4:GFP signal

9   localizes ubiquitously on the plasma membrane of the cells in which PIN4:GFP signal is present,

10   indicating that the regulation of PIN4:GFP by *EXO70A3* does not lead to a difference at the

11   sub-cellular level. This increase of the PIN4:GFP signal in root tips was also observed in lateral

12   roots although PIN4:GFP signal was absent in early stage lateral roots (Figure S4B). In contrast to

13   the *EXO70A3ox* line, *PIN4:GFP* level was significantly decreased in columella cells but not in the

14   stele of *CRISPR-exo70A3-1 PIN4::PIN4:GFP* plants (Figure 4A, B), supporting the idea that

15   *EXO70A3* specifically regulates PIN4 localization in columella cells.

16   While the function of *EXO70A3* in exocytosis suggests that the effect on PIN4 is exerted at the

17   protein level, we wanted to test this assumption. For this, we measured PIN4 transcript level in

18   *EXO70A3ox* plants. PIN4 transcript level was not elevated in root tips of these plants (Figure

19   S3G), further suggesting regulation of PIN4 by EXO70A3 at the protein level. To directly test this,

20   we conducted Fluorescence Recovery After Photobleaching (FRAP) experiments determining the

1   exocytosis rate of PIN4. Providing further evidence for the involvement of *EXO70A3* in the

2   exocytosis of PIN4, we found that the overexpression of *EXO70A3* results in the rapid recovery of

3   PIN4:GFP signal on the plasma membrane after photo-bleaching compared to the wildtype

4   background (Figure 4C).

5   Next we wanted to investigate the effect of EXO70A3 function on auxin transport. For this, we

6   compared expression patterns of the auxin responsive *DR5::GFP* reporter gene between wildtype,

7   *CRISPR-exo70A3-1* and *EXO70A3ox.* We found that there is an inverse relation between

8   PIN4:GFP and DR5::GFP signal intensities in wildtype, *CRISPR-exo70A3-1* and *EXO70A3ox*

9   backgrounds (Figure 4B, D). This suggests that *EXO70A3* modifies auxin levels in root tips

10   through the regulation of PIN4 levels in Columella tissue. Taken together, these results indicate

11   that EXO70A3 specifically regulates PIN4 presence in columella cells, presumably by a process

12   related to PIN4-specific exocytosis, and thereby regulates auxin distribution in root tips.

13

14   **Perturbation of *EXO70A3* specifically delays root growth responses to gravistimuli**

15   Since we had aimed to identify mechanisms that potentially alter RSA by modulating auxin

16   pathway, we tested the effect of knockout and overexpression of *EXO70A3* on various auxin

17   pathway-related phenotypes including other RSA traits, primary root length and lateral root density.

18   We did not find evidence for an effect in the two knockout mutants of *EXO70A3* and the two

19   *EXO70A3* ubiquitously overexpressing lines while testing primary root length, root growth

20   response to IAA, lateral root density, and auxin-dependent shoot traits (Figure S5A-D).

10

1   In contrast, in line with the result that *EXO70A3* mutants visibly altered root growth orientation of

2   seedlings in the presence of NPA (Figure 3A), an assay of dynamic root gravitropic responses in

3   the absence of the chemical treatment revealed that roots of the *EXO70A3* mutant lines show

4   significant delays in gravitropic responses compared to the wildtype (Figure 5A-D, Movie S1). We

5   therefore conclude that *EXO70A3* specifically regulates ARD but not, at least not to a detectable

6   extent, other auxin-dependent traits.

7   Even in the root tip, auxin is involved in multiple processes that could have an effect on root

8   growth orientation. We therefore investigated possible causes and first tested whether aberrant

9   development of the root meristem could be the cause for phenotypes. This is not true since

10 neither the cellular root architecture nor the numbers of gravity perceiving statocyte and statoliths

11 in the columella cells are altered in plants of the *EXO70A3* knockout and overexpression lines

12 (Figure S5A-D). Instead, and in line with the altered PIN4 distribution in these lines (Fig. 4A), the

13 *EXO70A3* knockout and overexpression lines showed a perturbation of the auxin distribution

14 pattern, as an asymmetric accumulation of DR5::GFP signal in the downward peripheral layer was

15 observed under gravistimulus in WT plants but not, in most cases (8/11 and 14/20 roots), in

16 *CRISPR-exo70A3-1* and *EXO70A3ox* plants, respectively (Figure 4E). Knockouts and

17 overexpressors of *EXO70A3* showed similar phenotypes, indicating that deregulation of the

18 *EXO70A3* function causes the phenotype. This is supported by the effect on DR5:GFP since both

19 knockout and overexpression of EXO70A3 causes perturbation of auxin responses. Such

20 similarities between overexpression and knockout (knockdown) mutants are frequently observed

11

1   as shown in a systematic screen in yeast in which 23% of the observed morphological

2   consequences upon gene overexpression were similar to the respective deletion mutant

3   phenotypes (Sopko *et al.*, 2006).

4   The prominent regulation of PIN4 by *EXO70A3* prompted us to investigate the role of *PIN4* in the

5   control of root growth orientation. Much like the EXO70A3 overexpression and mutant lines,

6   *pin4-3* knockout mutants did not show developmental phenotypes in shoot and root (Figure S5E).

7   While the dynamic root gravitropic response was also similar to Col-0 (Figure 5E), the variation of

8   root tip angles during the dynamic root gravitropic response, which is another index of root

9   agravitropism (Yamamoto *et al.*, 1998), was significantly larger than that of Col-0 (Figure S5F).

10   The cross of *EXO70A3ox* and *pin4-3* showed this variance phenotype (Figure S5F) of the pin4-3

11   mutant but did not display the *EXO70A3ox* induced change in the average dynamic root

12   gravitropic response (Figure 5E). This indicates that EXO70A3 is upstream of *PIN4*. Taken

13   together, this suggests that much like in overexpressors of *EXO70A3* and *CRISPR-exo70A3*

14   mutants, the control of gravitropism is exerted less precisely in *pin4-3* mutants, but that a more

15   pronounced disturbance of the quick root gravitropism requires an abnormal localization of PIN4

16   rather than absence of PIN4. Moreover, additional genes downstream of *EXO70A3* might be

17   needed to delay gravitropic responses.

18   Importantly, the effects of *EXO70A3* knockout and overexpression on ARD were consistent with

19   the phenotypic difference observed between natural alleles of *EXO70A3* (haplogroup H showed a

20   delay in responding to a gravistimulus (*EXO70A3* mutant type phenotype), population structure

12

1 corrected association test for angle changes at 10h after re-orientation: *p*-value = 0.037, Figure 5F,

2 Movie S2), suggesting that allelic variation of *EXO70A3* is involved in ARD processes. While the

3 delay in dynamic ARD was consistent with that observed in *CRISPR-exo70A3-1* and *EXO70A3ox*

4 plants, no differences in *EXO70A3* expression were observed between the haplogroups (Figure

5 S3I), suggesting that allelic differences are due to post-transcriptionally effective or coding

6 variation in the EXO70A3 protein itself. This notion is strengthened by the presence of

7 non-synonymous amino acid substitutions in haplogroup H and its causality in NPA response

8 variation (Figure 3B, S2B).

9

10 **_EXO70A3_ can shift root system architectures from shallow to deep**

11 We have shown that *EXO70A3* regulates RSA-related root traits on MS medium, which is not a

12 root growth substrate in nature. To assess the role of *EXO70A3* activity in physiologically relevant

13 conditions, we measured RSA of mature plants grown in soil. For this, we contemplated the space

14 the roots occupy particularly in a soil volume. The RSA of *CRISPR-exo70A3-1* and *EXO70A3ox*,

15 as well as that of *pin4-3*, showed a significantly higher extent of vertical expansion (decreased

16 shallowness; ANOVA: *p*-value = 1.1×10^{-3}, post-hoc Tukey test: *p*-value < 5.0×10^{-3}) in

17 comparison to the RSA of Col-0 (Figure 6A-C). Likewise, the *EXO70A3* locus of haplogroup H

18 was significantly associated with an increased vertical expansion of RSA compared to haplogroup

19 C (population structure corrected association test: *p*-value = 8.8×10^{-5}, Figure 6B, D). These data

20 strongly suggest that allelic variation of *EXO70A3* determines natural variation of RSA

13

1 configurations in soil, and depending on the *EXO70A3* allele conferring shallow rooting or deep

2 rooting. Interestingly, while *pin4-3* did not show the pronounced delay of gravitropic bending, it did

3 show deeper RSA. This might indicate that the heterogeneity of root angles during bending

4 observed in *pin4-3* and the *EXO70A3* mutants, rather than the quickness of the bending response

5 that is only observed in *EXO70A3* mutants leads to deeper rooting.

6

Shallow RSA-type *EXO70A3* leads to increased fitness in drought conditions

8 Given the remarkable tuning of root traits associated with natural alleles of *EXO70A3*, we

9 hypothesized that this locus is involved in local adaptation. To test this, we exploited data of

10 previous genome-wide scans for signatures of selection (Horton *et al.*, 2012) and climate

11 adaptation (Hancock *et al.*, 2011). Notably, we found a significant signature within the *EXO70A3*

12 haplotype block (CLR (Kim *et al.*, 2007), *p*-value < 0.01, Figure S2, S6A), suggesting a recent

13 selective sweep at this locus. Importantly, we also observed that, in SNP-climate condition

14 correlations that were caluculatd in Hacock *et al.*, 2011, the negative correlation between the SNP

15 in *EXO70A3* for which we detected the GWA signal with horizontality and the intensity of

16 precipitation seasonality (WorldClim, http://www.worldclim.org/) was significantly strong (Figure

17 S6B, included in top 5% SNPs). Since this parameter is a measure of the variability in weekly

18 precipitation throughout the year, we reasoned that this correlation might reflect adaptation to

19 temporal drought during the growth period of *A. thaliana.* To test this hypothesis, we assessed

20 whether allelic variation in *EXO70A3* affects fitness under water-limited conditions. Using seed

1   yield as a proxy for fitness, we observed that total seed numbers per plant in control conditions

2   was statistically indistinguishable in *EXO70A3ox* (Welch t-test *p*-value = 0.107) and haplogroup H

3   (ANOVA Haplotype *p*-value = 0.994) from Col-0 and haplogroup C, respectively (Table S3, Figure

4   7A). In drought conditions, however, it was significantly lower in *EXO70A3ox* (Welch t-test *p*-value

5   = 0.008) and haplogroup H (ANOVA *p*-value = 1.9×10^{-5}, population corrected association test

6   between C and H haplogroups was marginally significant: *p*-value = 0.052) as compared to Col-0

7   and haplogroup C, respectively (Table S3, Figure 7B). Moreover, while both Col-0 and

8   *EXO70A3ox* plants produced significantly fewer seeds in response to drought in comparison to

9   well-watered control conditions (Table S3, two-way ANOVA drought treatment: *p*-value < 2.0 $\times$

10   10^{-16}), *EXO70A3ox* responded more strongly to the drought treatment, showing a larger reduction

11   in seed number than Col-0 (Table S3, Figure 7C, two-way ANOVA genotype-treatment interaction:

12   *p*-value = 3.4×10^{-13}). Similarly, seed production of accessions in both haplogroup H and

13   haplogroup C was significantly reduced in response to drought treatment (Table S3, two-way

14   ANOVA drought treatment: *p*-value < 2.0×10^{-16}), yet haplogroup H was associated with a greater

15   reduction of seed number in response to drought (Table S3, Figure 7C, two-way ANOVA

16   genotype-treatment interaction: *p*-value < 2.0×10^{-16}, population structure corrected association

17   test for the response was marginally significant: *p*-value = 0.093). Therefore, the fitness

18   advantage conferred by haplotype C under water-limited conditions is consistent with its

19   correlation with precipitation seasonality. In summary, our data suggest that the haplogroup C

20   allele of *EXO70A3* might have contributed to the adaptation of *A. thaliana* to environments with

15

1   temporally variable water availability by tuning the RSA to a horizontally-expanded formation.

2

3   **DISCUSSION**

4   **Natural variation of auxin transport dependent early root growth traits**

5   Auxin signaling is a major regulatory pathway for root developmental processes such as cellular

6   proliferation and differentiation (Dello Ioio *et al.*, 2008; Ishida *et al.*, 2010), cellular expansion

7   (Muday *et al.*, 2012), root growth direction (Band *et al.*, 2012), and lateral root formation (Lavenus

8   *et al.*, 2013); these traits are critical for determining root system architecture. Despite the

9   prominent role of the auxin pathway in regulating root growth and recent progress in revealing

10   genetic bases of natural variation of root growth (Gifford *et al.*, 2013; Meijon *et al.*, 2014; Slovak *et*

11   *al.*, 2014; Satbhai *et al.*, 2018), it remained unclear whether and how the auxin pathway itself is

12   subject to natural variation. Here we demonstrated that there is significant natural variation in

13   response to perturbation of auxin transport for root growth orientation control, one trait regulated

14   by auxin-controlled processes. While the change of root length in different accessions upon auxin

15   transport perturbation was rather homogenous, the change of root growth orientation displayed a

16   much higher variability (Figure 1B, S1). It is therefore tempting to speculate that the auxin

17   pathway-related components that govern root growth orientation are subject to natural variation to

18   a higher extent than those that govern root growth rate. It follows that auxin-dependent regulatory

19   mechanisms of root elongation and root growth orientation are independent. This idea is

20   consistent with recent work that has shown that the change of root growth direction in response to

16

1   gravity stimuli is mediated by rapid changes in auxin fluxes, while these rapid changes do not

2   affect auxin dependent root apical meristem zonation (Mahonen *et al.*, 2014).

3

4   **Sequence variation at the *EXO70A3* locus determines how roots respond to gravity**

5   Using GWA mapping and subsequent genetic and molecular analyses, we determined that

6   *EXO70A3* is the causal locus that underlies a significant proportion of the response in terms of

7   root growth orientation to auxin transport inhibition. We base this conclusion on multiple lines of

8   evidence. First, this gene is in a haplotype block centered around the marker SNP which showed

9   the highest signal of association (Figure S2), and according to the 1001 genome sequencing

10   project (1001genomes.org), the high response of haplogroup H to NPA is linked with

11   non-synonymous amino acid changes that were exclusively found in the *EXO70A3* coding region

12   of this group (Figure S2). Indeed, alleles containing this non-synonymous polymorphism were

13   causal for the variable response of natural accessions to NPA (Figure 3B). In addition, the

14   expression pattern of *EXO70A3* in the root is specific to tissues with key functions in root growth

15   direction control (Figure 2B, S3A-E). Moreover, natural alleles as well as abnormal distribution of

16   EXO70A3 affect root orientation responses (Figure 5). Furthermore, *EXO70A3* is functionally

17   linked to auxin transport regulation that is relevant to root orientation control at the cellular and

18   molecular level. Overexpression of *EXO70A3* results in overaccumulation of PIN4 in columella

19   cells and *exo70a3* knockout eliminated PIN4:GFP signal from columella cells, altering auxin signal

20   localization patterns during root gravitropism (Figure 4A-D). Since the mRNA expression level of

17

1 PIN4 in *EXO70A3ox* is indistinguishable from that of Col-0 wildtype (Figure S3H), EXO70A3 is an

2 exocytosis factor (Synek *et al.*, 2006), and *EXO70A3* level corresponds with PIN4-GFP signal

3 level, it is highly likely that EXO70A3 regulates the abundance and localization of PIN4 at the

4 plasma membrane. Consistent with this model, FRAP analysis demonstrated the involvement of

5 *EXO70A3* in PIN4 exocytosis (Figure 4C). In sum, these results suggest that EXO70A3 regulates

6 plasma membrane localization of PIN4 by exocytosis and thereby determines root gravitropic

7 responses (Figure S7). The non-synonymous amino acid changes in different natural *EXO70A3*

8 alleles would affect this process and eventually cause the natural variation observed in the

9 modulation of the gravitropic response by NPA (Figure 1A). A detailed RNA-Seq analysis in root

10 cells showed that the highest expression of *EXO70A3* in the data set was detected under

11 cycloheximide treatment (Li *et al.,* 2017, Figure S3E), suggesting that *EXO70A3* is tightly

12 regulated by protein degradation. This might indicate that the regulation of related components

13 including auxin signaling factors and auxin transporters such as PINs at protein level might play

14 important roles in the rapid response of roots to gravistimuli.

15

16 **The auxin pathway can be specifically modulated by a component of the exocytosis**

17 **pathway**

18 We have identified a mechanism which controls the auxin pathway and establishes variation in

19 RSA configurations via modulation of the auxin transport machinery. Interestingly, despite the

20 well-known contributions of auxin efflux carriers and endocytosis factors to auxin transport, we did

18

1   not identify any of the known auxin transporters and endocytosis factors. Instead, we identified a

2   component of the exocytosis pathway. In comparison with intensely studied auxin carriers and

3   endocytic regulators for auxin transport (Kleine-Vehn and Friml, 2008), exocytic components have

4   not been regarded as of primary importance (Kleine-Vehn *et al.*, 2011) although the involvement

5   of several general exocytosis factors in the transport of PIN proteins has been recently reported

6   (Feraru *et al.*, 2012; Hazak *et al.*, 2010; Naramoto *et al.*, 2014; Tanaka *et al.*, 2014). In particular,

7   the involvement of the *EXOCYST* family has not been well investigated despite the remarkable

8   radiation of family members of EXOCYST-subunit encoding genes in landplants (Cvrckova *et al.*,

9   2012). Of these, only the role of the ubiquitous *A. thaliana* exocytosis factor, *EXOCYST70A1*, in

10   general cellular recycling had been shown to involve regulation of the PIN1 and 2 auxin

11   transporters, thereby affecting numerous traits including shoot and root phenotypes (Drdova *et al.*,

12   2013). Moreover, the importance of EXOCYSTs in auxin transport and signaling is still debated

13   (Cole *et al.*, 2014). Our data show a clear and specific role of an EXOCYST complex component,

14   EXO70A3 on auxin-dependent growth through the regulation of PIN4 localization. The specific

15   function of *EXO70A3* detailed here is consistent with the model that specific EXOCYST

16   complexes containing a particular EXOCYST70 isoform can have distinct tissue- or

17   process-specific roles in land plants. While the genetic perturbation of many auxin pathway genes

18   leads to severe and often highly pleiotropic effects on multiple traits (Friml *et al.,* 2002; Tsugeki *et*

19   *al.,* 2009), *EXO70A3* represents an uncharted layer of the regulation of auxin signaling system

20   that modulates the swiftness of auxin-dependent control of the root gravitropism by conferring the

19

1   flexibility of auxin transport through PIN4 without significantly disrupting the auxin pathway itself in

2   root tips.

3

4   **EXO70A3 controls root system architecture, providing adaptive value for drought**

5   **conditions**

6   Our data strongly suggest that *EXO70A3*-dependend variation in the control of root growth

7   direction can result in either a shallow or a deep RSA (Figure 6). A major part of the function of

8   *EXO70A3* is exerted by its downstream target PIN4 as lack of *PIN4* in the *pin4-3* mutant leads to a

9   deeper RSA in a same way as dysregulation of *EXO70A3* does. As *pin4-3* plants showed the

10   increased variation of root tip angles while it did not show the delay of gravitropic root bending, it

11   is indicated that downward growth of roots in the soil does not simply reflect the rapidness of

12   bending upon gravity change on agar plates. There are various other stimuli that regulate root

13   growth directions in the soil in addition to gravistimulus. Functions of *EXO70A3* in response to

14   these stimuli in collaboration with that to gravistimulus might fully explain RSA formation in the

15   soil.

16   The distribution of the *EXO70A3* alleles is highly associated with precipitation seasonality, the

17   variability in weekly precipitation throughout the year (Figure S6B). Importantly, plants with

18   different RSA configurations conferred by variation of the *EXO70A3* locus seem to display

19   different fitness in environments with variable rainfall patterns (Figure S7). In particular, our data

20   indicate a beneficial effect of a shallow, more horizontally distributed RSA in *A. thaliana* under

1   drought conditions. Since surface soil water is considered to be important in environments with

2   sparse rainfall (Lauenroth *et al.*, 2014; Nippert and Knapp, 2007), a shallow root system might be

3   an adaptation for efficiently capture the water in the short time that it is available. This idea is

4   consistent with findings that, in water-limited ecosystems, there are significant positive

5   correlations between precipitation seasonality and rooting shallowness in annual species (Schenk

6   and Jackson, 2002) and between highly-branched (rather than deep) root systems and

7   drought-tolerance of grass species (Hartnett *et al.*, 2013). However, it has been recently reported

8   that *DEEPER ROOTING 1*, an auxin inducible gene of *Oryza sativa*, contributes to drought

9   tolerance through vertically deeper RSA formation (Uga *et al.*, 2013). In contrast to *A. thaliana*,

10   which often grows in areas of highly variable rainfall, rice is cultivated at relatively high

11   temperatures on irrigated soil. Therefore, the differences in RSA observed between these species

12   might reflect contrasting strategies for adaptation to environments with different water-limitation

13   constraints.

14

15   **GWA mapping can uncover novel players with adaptive relevance**

16   Despite the fact that the auxin pathway is one of the most highly investigated signaling pathways

17   in plants, we found no significant associations with loci in proximity of known auxin pathway

18   components. While false negatives can be expected due to our approach (in particular the limited

19   number of accessions as well as the stringent population structure control and statistical

20   threshold), this still suggests that the common alleles mapped by GWA studies using phenotypic

21

1   variation in natural populations are typically not the large-effect genes that are frequently mapped

2   by mutant approaches. This is in agreement with other root GWA studies in which unbiased

3   approaches were taken to map genes. For instance, despite the large body of work for nitrogen

4   responses of roots based on mutant approaches, recent GWA studies of natural variation in

5   nitrogen-level dependent root growth responses (Gifford *et al.*, 2013) exclusively identified genes

6   which had not been attributed to a function in this process based on past studies. The same

7   pattern holds true for root growth regulation at the cellular scale (Meijon *et al.*, 2014) and the

8   organ level (Lachowiec *et al.*, 2015; Slovak *et al.*, 2014). Finally, a recent GWAS study showed

9   that genes known for their involvement in the abscisic acid hormonal pathway were not enriched

10   in the large number of genes associated with root growth responses to the hormone abscisic acid

11   (Ristova *et al.*, 2018). A reason for the absence of known genes could be that alterations of the

12   expression or function of genes that are critically important for fundamental processes in

13   development cause drastic effects with pleiotropic consequences, causing detrimental effects for

14   the plants. Such alleles are likely not commonly maintained in a natural population. Therefore,

15   with regard to understanding the genetic components that determine phenotypes (the genotype to

16   phenotype challenge) and are of adaptive relevance, mapping of these natural alleles seems to

17   be a highly promising approach. Overall, our findings not only demonstrate a specific role of

18   exocytosis in the modulation of auxin-dependent developmental processes, but also underscore

19   the importance of processes related to auxin pathway for the natural variation of RSA. The

20   investigation of other exocytosis components promises to elucidate precise and dynamic control

22

1   mechanisms of auxin dependent plant growth processes.

2

3   **EXPERIMENTAL PROCEDURES**

4

5   **Plant materials and growth conditions**

6   All plants for image acquisition on plates were grown on vertical 1 × MS agar plates (1 % sucrose,

7   0.8 % agar, pH = 5.7) in 12 cm × 12 cm square plates with or without chemicals under long day

8   conditions (16 hours light) at 21°C. The seeds of the 215 natural accessions of *Arabidopsis*

9   *thaliana* (Table S1) were a gift from Dr. Magnus Nordborg's laboratory (GMI, Vienna, Austria).

10   *EXO70A3ox* (SALK_075426) were purchased from Nottingham Arabidopsis Stock Center

11   (Leicestershire, UK). Two CRISPR knockout lines (*CRISPR-exo70A3-1* and *CRISPR-exo70A3-2*)

12   were created following a previously published method (Mao *et al.*, 2016). *PIN1-GFP, PIN2-GFP,*

13   *PIN3-GFP, PIN4-GFP, PIN7-GFP, pin4-3* and *DR5::GFP* were a gift from Dr. Jürgen Kleine-Vehn

14   (University of Natural Resources and Life Sciences, Vienna, Austria). Crosses between

15   *CRISPR-exo70A3-1, EXO70A3ox* and other mutants were made by manually pollinating

16   emasculated pistils of those marker lines with pollen of these *EXO70A3* mutants. For allelic

17   complementation lines, protein coding genetic sequences of *EXO70A3* were amplified from

18   various natural accessions and fused with *EXO70A3* promoter sequence from Col-0, then

19   transformed to *CRISPR-exo70A3-1*. Plants for crosses, seed amplification, and phenotyping of

20   aerial parts were grown on soil at 21°C, 16 hours light/16°C, 8 hours dark conditions.

23

1

Quantitative phenotyping of NPA treated roots and GWA study

The 215 natural accessions were grown on 1 × MS agar plates containing 10 μM NPA under long day conditions (16 hours light) at 21°C. 24 plants were seeded for each accession. Starting at 2 days after germination (DAG), root images were acquired by scanners (EPSON Perfection V600 Photo, Seiko Epson CO., Nagano, Japan) each 24 hours for 5 days (2 DAG – 6 DAG). Root image analyses and phenotype quantification were performed using the BRAT software (Slovak *et al.*, 2014). GWA studies were conducted using the average trait value for each trait of 215 natural accessions by an accelerated mixed model (EMMAX (Kang *et al.*, 2010)) followed by EMMA (Kang *et al.*, 2008) for the most significant 200 associations as implemented in the web-based GWA mapping application GWAPP (Seren *et al.*, 2012, conducted on December 15, 2014).

Data mining and genetic analysis

The eFP browser (Winter *et al.*, 2007) was used as a general reference for gene expression profiles of candidate genes. SNP data obtained from the *Arabidopsis thaliana* 1001 genome project (Schmitz *et al.*, 2013, www.1001genomes.org) was used to analyze polymorphism among natural accessions. The analysis regarding signals of selection was conducted using the Selection Browser of the Regional Mapping Project (Horton *et al.*, 2012). In haplogroup analysis, grouping of the 215 natural accessions of *A. thaliana* was performed according to haplotypes around the SNPs in a 40KB window around the SNPs of interest. These SNPs were used as the

24

1   input for fastPHASE (Scheet and Stephens, 2006) version 1.4.0 and visualized using R script.

2

3   **Plant observations**

4   For root phenotyping of *CRISPR-exo70A3-1*, *CRISPR-exo70A3-2*, *EXO70A3ox*,

5   *35S::GFP:EXO70A3*, *pin4-3* and *pin4-3 EXO70A3ox* young seedlings, seedlings were grown on 1

6   × MS agar plates. For root angle changes of these mutants or allelic complementation lines in

7   response to NPA, plants grown for five days after germination were transferred to 1 × MS agar

8   plates with or without 0.5 μM or 0.1 μM NPA, respectively, and images were acquired by scanners

9   (EPSON Perfection V600 Photo) one day after the transfer and analyzed using Fiji (Schindelin *et*

10   *al.*, 2012). For each genotype, 10 or more plants were used. For the observation of statocytes,

11   plants were grown on 1 × MS agar plates for five days after germination and stained in Lugol's

12   solution for two minutes and transferred into a chloral hydrate solution. Images were acquired

13   using an AXIO image.M1 or an AXIO observer Z1 (Carl Zeiss AG, Oberkochen, Germany) and a

14   CMOS camera (SPOT Idea 1.3 Mp Color Digital Camera, SPOT imaging, Sterling Heights, MI,

15   USA). 5 - 10 plants per genotype were observed in an experiment. For analysis of above-ground

16   organs of mature plants, images were acquired using a Nikon D80 (Nikon Co., Tokyo, Japan)

17   digital camera. 4 - 9 plants were observed for each line. For analyses of fluorescent protein

18   containing lines, crossbred lines and control lines for these crossbreds were grown on 1 × MS

19   agar plates with or without 1 μM NPA for six days after germination. GFP signals in plant roots

20   were observed under a confocal microscope Zeiss LSM700 (Carl Zeiss) with a 10× objective (EC

1   plan Neofluar 10×0.3 M27), a 20× objective (Plan Apochromat 20×0.8 M27) or a 40× objective

2   (Plan-Apochromat 40×/0.95 Korr M27, Zeiss). FRAP (Fluorescent recovery after photo bleaching)

3   was conducted using *PIN4::PIN4:GFP* and *PIN4::PIN4:GFP EXO70A3ox* lines using a Visitron

4   Spining Disc microscope, which is based on Nikon Eclipse Ti E inverted microscope (Nikon

5   Instech Co., Ltd., Tokyo, Japan) equipped with CSU-W1 spinning disc unit (Yokogawa Electric

6   Corporation, Tokyo, Japan), with a 60× water objective (Plan Apo VC 60×/1.2 WI water, Nikon)

7   and Immersol WTM (Carl Zeiss). At least ten plants per genotype were observed for an

8   experiment. To compare traits between haplogroups, we used eight accessions (haplogroup C:

9   Ler-1, Shakdara (Sha), Lp2-2, and Per-1; haplogroup H: LAC-5, MIB-60, Coc-1, and Ty-0). All

10 experiments were repeated at least twice.

11

12 **Root system architecture (RSA) assay**

13 RSA in soil was studied using three plants from each genotype and in a blind fashion, so that the

14 plant genotypes were not known to the researcher conducting the test. Each plant was grown on

15 soil for 30 days in a pot (ϕ 20 cm, 17 cm height) at 21°C, 16 hours light/16°C, 8 hours dark

16 conditions. The whole pot was then sectioned in two halves at the center of the plant and an RSA

17 image was acquired by a Nikon D80 camera. Using Fiji, the roots on the image were marked

18 (overlay) and subsequently the coordinates of all root pixels were determined. The Shallowness

19 (standard deviation of all root pixels in X axis direction in a picture divided by that in Y axis

20 direction) was calculated using these data as an indicator of shallow or deep RSA.

1

Seed number assay

3 As a proxy of fitness in drought conditions, we measured seed number/plant for 8 natural

4 accessions, Col-0 and *EXO70A3ox*. We used four plants from each genotype and four sets of the

5 whole drought experiment. The experiment was conducted blindly so that the plant genotypes

6 were not known to the researcher conducting the test. Four plants of a line were grown on soil for

7 more than 60 days in a pot (ϕ 20 cm, 17 cm height) at 60% humidity, 21°C, 16 hours light/16°C, 8

8 hours dark conditions until seed production was completed. Four plants of two different genotypes

9 were grown within one pot. In drought conditions, the water content of pots was decreased from

10 60% (Day After Germination: DAG5) to 30% (DAG 35). After that, the water content was kept at

11 25 %. For the water-sufficient control, the same experiment was repeated while water level was

12 kept at 65% through the whole experimental period. Mature siliques from each plant were

13 harvested and the number of seeds in five siliques was counted to determine the average number

14 of seeds per silique for each plant. Subsequently, the total silique number of each plant was

15 counted and the total seed number was calculated using the average seed number per silique and

16 the total silique number. An average value of four plants of each line in a pot was calculated,

17 rounded and used in statistical analyses. Significance of the difference in drought responses was

18 calculated using Poisson regression models.

19

20 **Quantitative reverse transcription PCR (qrt-PCR)**

1   For qrt-PCR, plants were grown on 1 × MS agar plates under normal growth conditions with or

2   without 10 μM NPA or 100 nM IAA for 7 days after germination. Tissues were collection by

3   excision with fine scissors. For root tips, 2.5 mm root tips were excised from primary roots. 10

4   plants for the whole plant, 10 plants for the shoot, 20 plants for the root, and more than 150 plants

5   for the root tip samples were used. Samples were immediately frozen in liquid nitrogen, ground,

6   and total RNA was extracted using the RNeasy Plant Mini kit (QIAGEN GmbH, Hilden, Germany).

7   qrt-PCR reaction was prepared using 2x SensiMix[TM] SYBR & Fluorescein Kit (PEQLAB LLC,

8   Wilmington, DE, USA) and PCR was conducted with a combination of iCycler and IQ5 (Bio-Rad

9   Laboratories, Inc., Hercules, CA, USA). All transcript levels were normalized to the tubulin β gene

10   (AT5G62690) or 18S ribosomal RNA. All experiments were repeated at least twice. Genes

11   quantified include *EXO70A3* (AT5G52350), AT5G52340, AT5G52360, PIN1 (AT1G73590), PIN2

12   (AT5G57090), PIN3 (AT1G70940), PIN4 (AT2G01420), and PIN7 (AT1G23080). For the

13   comparison of *EXO70A3* expression levels among natural accessions, we used eight accessions

14   (haplogroup C: Ler-1, Shakdara (Sha), Lp2-2, and Per-1; haplogroup H: LAC-5, MIB-60, Coc-1,

15   and Ty-0).

16

17   **ACKNOWLEDGEMENTS**

28

16

REFERENCES

Algeo, T. J., and Scheckler, S. E. (1998). Terrestrial-marine teleconnections in the Devonian: links between the evolution of land plants, weathering processes, and marine anoxic events. Philos T R Soc B *353*, 113-130.

Atkinson, J. A., Rasmussen, A., Traini, R., Voss, U., Sturrock, C., Mooney, S. J., Wells, D. M., and Bennett, M. J. (2014). Branching Out in Roots: Uncovering Form, Function, and Regulation. Plant Physiol *166*, 538-550.

Band, L. R., Wells, D. M., Larrieu, A., Sun, J. Y., Middleton, A. M., French, A. P., Brunoud, G., Sato, E. M., Wilson, M. H., Peret, B.*, et al.* (2012). Root gravitropism is regulated by a transient lateral auxin gradient controlled by a tipping-point mechanism. P Natl Acad Sci USA *109*, 4668-4673.

Benfey, P. N., and Scheres, B. (2000). Root development. Curr Biol *10*, R813-R815.

Benjamins, R., and Scheres, B. (2008). Auxin: The looping star in plant development. Annu Rev Plant Biol *59*, 443-465.

Brady, S. M., Orlando, D. A., Lee, J. Y., Wang, J. Y., Koch, J., Dinneny, J. R., Mace, D., Ohler, U., and Benfey, P. N. (2007). A high-resolution root spatiotemporal map reveals dominant expression

patterns. Science *318*, 801-806.

Cole, R. A., McInally, S. A., and Fowler, J. E. (2014). Developmentally distinct activities of the exocyst enable rapid cell elongation and determine meristem size during primary root growth in *Arabidopsis*. Bmc Plant Biol *14*, 386.

Cvrckova, F., Grunt, M., Bezvoda, R., Hala, M., Kulich, I., Rawat, A., and Zarsky, V. (2012). Evolution of the land plant exocyst complexes. Front Plant Sci *3*, 159.

De Rybel, B., Audenaert, D., Beeckman, T., and Kepinski, S. (2009). The Past, Present, and Future of Chemical Biology in Auxin Research. Acs Chem Biol *4*, 987-998.

Dello Ioio, R., Nakamura, K., Moubayidin, L., Perilli, S., Taniguchi, M., Morita, M. T., Aoyama, T., Costantino, P., and Sabatini, S. (2008). A Genetic Framework for the Control of Cell Division and Differentiation in the Root Meristem. Science *322*, 1380-1384.

Den Herder, G., Van Isterdael, G., Beeckman, T., and De Smet, I. (2010). The roots of a new green revolution. Trends Plant Sci *15*, 600-607.

Drdova, E. J., Synek, L., Pecenkova, T., Hala, M., Kulich, I., Fowler, J. E., Murphy, A. S., and

Zarsky, V. (2013). The exocyst complex contributes to PIN auxin efflux carrier recycling and polar auxin transport in *Arabidopsis*. Plant J *73*, 709-719.

Feraru, E., Feraru, M. I., Asaoka, R., Paciorek, T., De Rycke, R., Tanaka, H., Nakano, A., and Friml, J. (2012). BEX5/RabA1b Regulates trans-Golgi Network-to-Plasma Membrane Protein Trafficking in *Arabidopsis*. Plant Cell *24*, 3074-3086.

Friml, J., Benkova, E., Blilou, I., Wisniewska, J., Hamann, T., Ljung, K., Woody, S., Sandberg, G., Scheres, B., Jurgens, G., and Palme, K. (2002). AtPIN4 mediates sink-driven auxin gradients and root patterning in *Arabidopsis*. Cell *108*, 661-673.

Gibling, M. R., and Davies, N. S. (2012). Palaeozoic landscapes shaped by plant evolution. Nat Geosci *5*, 99-105.

Gifford, M. L., Banta, J. A., Katari, M. S., Hulsmans, J., Chen, L., Ristova, D., Tranchina, D., Purugganan, M. D., Coruzzi, G. M., and Birnbaum, K. D. (2013). Plasticity Regulators Modulate Specific Root Traits in Discrete Nitrogen Environments. Plos Genet *9*.

Goda, H., Sasaki, E., Akiyama, K., Maruyama-Nakashita, A., Nakabayashi, K., Li, W. Q., Ogawa, M., Yamauchi, Y., Preston, J., Aoki, K., *et al.* (2008). The AtGenExpress hormone and chemical

32

treatment data set: experimental design, data evaluation, model data analysis and data access. Plant J *55*, 526-542.

Hancock, A. M., Brachi, B., Faure, N., Horton, M. W., Jarymowycz, L. B., Sperone, F. G., Toomajian, C., Roux, F., and Bergelson, J. (2011). Adaptation to Climate Across the *Arabidopsis thaliana* Genome. Science *334*, 83-86.

Hartnett, D. C., Wilson, G. T., Ott, J. P., and Setshogo, M. (2013). Variation in root system traits among African semi-arid savanna grasses: Implications for drought tolerance. Austral Ecol *38*, 383-392.

Hazak, O., Bloch, D., Poraty, L., Sternberg, H., Zhang, J., Friml, J., and Yalovsky, S. (2010). A Rho Scaffold Integrates the Secretory System with Feedback Mechanisms in Regulation of Auxin Distribution. PLoS Biol *8*, e1000282.

Hilson, P., Allemeersch, J., Altmann, T., Aubourg, S., Avon, A., Beynon, J., Bhalerao, R. P., Bitton, F., Caboche, M., Cannoot, B.*, et al.* (2004). Versatile gene-specific sequence tags for *Arabidopsis* functional genomics: Trancript profiling and reverse genetics applications. Genome Res *14*, 2176-2189.

Horton, M. W., Hancock, A. M., Huang, Y. S., Toomajian, C., Atwell, S., Auton, A., Muliyati, N. W., Platt, A., Sperone, F. G., Vilhjalmsson, B. J*., et al.* (2012). Genome-wide patterns of genetic variation in worldwide *Arabidopsis thaliana* accessions from the RegMap panel. Nat Genet *44*, 212-216.

Ishida, T., Adachi, S., Yoshimura, M., Shimizu, K., Umeda, M., and Sugimoto, K. (2010). Auxin modulates the transition from the mitotic cycle to the endocycle in *Arabidopsis*. Development *137*, 63-71.

Jung, J. K. H., and McCouch, S. (2013). Getting to the roots of it: genetic and hormonal control of root architecture. Front Plant Sci *4*, 186.

Kang, H. M., Sul, J. H., Service, S. K., Zaitlen, N. A., Kong, S. Y., Freimer, N. B., Sabatti, C., and Eskin, E. (2010). Variance component model to account for sample structure in genome-wide association studies. Nat Genet *42*, 348-354.

Kang, H. M., Zaitlen, N. A., Wade, C. M., Kirby, A., Heckerman, D., Daly, M. J., and Eskin, E. (2008). Efficient control of population structure in model organism association mapping. Genetics *178*, 1709-1723.

1 Kee, Y., Yoo, J. S., Hazuka, C. D., Peterson, K. E., Hsu, S. C., and Scheller, R. H. (1997). Subunit

2 structure of the mammalian exocyst complex. P Natl Acad Sci USA *94*, 14438-14443.

3

4 Kim, S., Plagnol, V., Hu, T. T., Toomajian, C., Clark, R. M., Ossowski, S., Ecker, J. R., Weigel, D.,

5 and Nordborg, M. (2007). Recombination and linkage disequilibrium in *Arabidopsis thaliana*. Nat

6 Genet *39*, 1151-1155.

7

8 Kleine-Vehn, J., and Friml, J. (2008). Polar Targeting and Endocytic Recycling in

9 Auxin-Dependent Plant Development. Annu Rev Cell Dev Bi *24*, 447-473.

10

11 Kleine-Vehn, J., Wabnik, K., Martiniere, A., Langowski, L., Willig, K., Naramoto, S., Leitner, J.,

12 Tanaka, H., Jakobs, S., Robert, S.*, et al.* (2011). Recycling, clustering, and endocytosis jointly

13 maintain PIN auxin carrier polarity at the plasma membrane. Mol Syst Biol *7*, 540.

14

15 Lachowiec, J., Shen, X., Queitsch, C., and Carlborg, O. (2015). A Genome-Wide Association

16 Analysis Reveals Epistatic Cancellation of Additive Genetic Variance for Root Length in

17 *Arabidopsis thaliana*. Plos Genet *11*, e1005541.

18

19 Lauenroth, W. K., Schlaepfer, D. R., and Bradford, J. B. (2014). Ecohydrology of Dry Regions:

20 Storage versus Pulse Soil Water Dynamics. Ecosystems *17*, 1469-1479.

1

2   Lavenus, J., Goh, T., Roberts, I., Guyomarc'h, S., Lucas, M., De Smet, I., Fukaki, H., Beeckman,

3   T., Bennett, M., and Laplaze, L. (2013). Lateral root development in *Arabidopsis*: fifty shades of

4   auxin. Trends Plant Sci *18*, 455-463.

5

6   Li, S., Yamada, M., Han, X., Ohler U., and Benfey P. N. (2016). High-Resolution Expression Map

7   of the *Arabidopsis* Root Reveals Alternative Splicing and lincRNA Regulation. Dev Cell *39*,

8   508-522.

9

10   Mahonen, A. P., ten Tusscher, K., Siligato, R., Smetana, O., Diaz-Trivino, S., Salojarvi, J.,

11   Wachsman, G., Prasad, K., Heidstra, R., and Scheres, B. (2014). PLETHORA gradient formation

12   mechanism separates auxin responses. Nature *515*, 125-129.

13

14   Mao, Y., Zhang, Z., Feng, Z., Wei, P., Zhang, H., Botella, J. R., and Zhu, J. K. (2016).

15   Development of germ-line-specific CRISPR-Cas9 systems to improve the production of heritable

16   gene modifications in *Arabidopsis*. Plant Biotec J. *14*, 519-532.

17

18   Masson, P. H., Tasaka, M., Morita, M. T., Guan, C., Chen, R., and Boonsirichai, K. (2002).

19   *Arabidopsis thaliana*: A Model for the Study of Root and Shoot Gravitropism. The Arabidopsis

20   Book, e0043.

Matern, H. T., Yeaman, C., Nelson, W. J., and Scheller, R. H. (2001). The Sec6/8 complex in mammalian cells: Characterization of mammalian Sec3, subunit interactions, and expression of subunits in polarized cells. P Natl Acad Sci USA *98*, 9648-9653.

Meijon, M., Satbhai, S. B., Tsuchimatsu, T., and Busch, W. (2014). Genome-wide association study using cellular traits identifies a new regulator of root development in *Arabidopsis*. Nat Genet *46*, 77-81.

Muday, G. K., Rahman, A., and Binder, B. M. (2012). Auxin and ethylene: collaborators or competitors? Trends Plant Sci *17*, 181-195.

Naramoto, S., Nodzynski, T., Dainobu, T., Takatsuka, H., Okada, T., Friml, J., and Fukuda, H. (2014). *VAN4* Encodes a Putative TRS120 That is Required for Normal Cell Growth and Vein Development in *Arabidopsis*. Plant Cell Physiol *55*, 750-763.

Nippert, J. B., and Knapp, A. K. (2007). Linking water uptake with rooting patterns in grassland species. Oecologia *153*, 261-272.

Ossowski, S., Schwab, R., and Weigel, D. (2008). Gene silencing in plants using artificial

37

1   microRNAs and other small RNAs. Plant J *53*, 674-690.

2

3   Peret, B., De Rybel, B., Casimiro, I., Benkova, E., Swarup, R., Laplaze, L., Beeckman, T., and

4   Bennett, M. J. (2009). *Arabidopsis* lateral root development: an emerging story. Trends Plant Sci

5   *14*, 399-408.

6

7   Petrasek, J., and Friml, J. (2009). Auxin transport routes in plant development. Development *136*,

8   2675-2688.

9

10   Pierik, R., and Testerink, C. (2014). The Art of Being Flexible: How to Escape from Shade, Salt,

11   and Drought. Plant Physiol *166*, 5-22.

12

13   Ristova, D., Giovannetti, M., Metesch, K., and Busch, W. (2018) Natural genetic variation shapes

14   root system responses to phytohormones in Arabidopsis. Plant J. *96*, 468-481

15

16   Satbhai, S. B., Setzer, C., Freynschlag, F., Slovak, R., Kerdaffrec, E., and Busch, W. (2017).

17   Natural allelic variation of FRO2 modulates *Arabidopsis* root growth under iron deficiency. Nat

18   Commun *8*:15603.

19

20   Scheet, P., and Stephens, M. (2006). A fast and flexible statistical model for large-scale population

1   genotype data: Applications to inferring missing genotypes and haplotypic phase. Am J Hum

2   Genet *78*, 629-644.

3

4   Schenk, H. J., and Jackson, R. B. (2002). Rooting depths, lateral root spreads and

5   below-ground/above-ground allometries of plants in water-limited ecosystems. J Ecol *90*,

6   480-494.

7

8   Schindelin, J., Arganda-Carreras, I., Frise, E., Kaynig, V., Longair, M., Pietzsch, T., Preibisch, S.,

9   Rueden, C., Saalfeld, S., Schmid, B*., et al.* (2012). Fiji: an open-source platform for

10   biological-image analysis. Nat Methods *9*, 676-682.

11

12   Schmid, M., Davison, T. S., Henz, S. R., Pape, U. J., Demar, M., Vingron, M., Scholkopf, B.,

13   Weigel, D., and Lohmann, J. U. (2005). A gene expression map of *Arabidopsis thaliana*

14   development. Nat Genet *37*, 501-506.

15

16   Schmitz, R. J., Schultz, M. D., Urich, M. A., Nery, J. R., Pelizzola, M., Libiger, O., Alix, A., McCosh,

17   R. B., Chen, H. M., Schork, N. J., and Ecker, J. R. (2013). Patterns of population epigenomic

18   diversity. Nature *495*, 193-198.

19

20   Seren, U., Vilhjalmsson, B. J., Horton, M. W., Meng, D. Z., Forai, P., Huang, Y. S., Long, Q.,

1   Segura, V., and Nordborg, M. (2012). GWAPP: A Web Application for Genome-Wide Association

2   Mapping in Arabidopsis. Plant Cell *24*, 4793-4805.

3

4   Slovak, R., Goeschl, C., Su, X., Shimotani, K., Shiina, T., and Busch, W. (2014). A Scalable

5   Open-Source Pipeline for Large-Scale Root Phenotyping of *Arabidopsis*. The Plant Cell Online,

6   www.plantcell.org/cg/doi/10.1105/tpc.1114.124032.

7

8   Sopko, R., Huang, D., Preston, N., Chua, G., Papp, B., Kafadar, K., Snyder, M., Oliver, S. G.,

9   Cyert, M., Hughes, T. R., Boone, C., and Andrews, B. (2006). Mapping Pathways and Phenotypes

10   by Systematic Gene Overexpression. Mol Cell *21*, 319-330.

11

12   Synek, L., Schlager, N., Elias, M., Quentin, M., Hauser, M. T., and Zarsky, V. (2006). AtEXO70A1,

13   a member of a family of putative exocyst subunits specifically expanded in land plants, is

14   important for polar growth and plant development. Plant J *48*, 54-72.

15

16   Tanaka, H., Nodzynski, T., Kitakura, S., Feraru, M. I., Sasabe, M., Ishikawa, T., Kleine-Vehn, J.,

17   Kakimoto, T., and Friml, J. (2014). BEX1/ARF1A1C is Required for BFA-Sensitive Recycling of

18   PIN Auxin Transporters and Auxin-Mediated Development in *Arabidopsis*. Plant Cell Physiol *55*,

19   737-749.

20

TerBush, D. R., Maurice, T., Roth, D., and Novick, P. (1996). The Exocyst is a multiprotein complex required for exocytosis in Saccharomyces cerevisiae. EMBO J *15*, 6483-6494.

Tsugeki, R., Ditengou, F. A., Sumi, Y., Teale, W., Palme, K., and Okada, K. (2009). NO VEIN Mediates Auxin-Dependent Specification and Patterning in the *Arabidopsis* Embryo, Shoot, and Root. Plant Cell *21*, 3133-3151.

Uga, Y., Sugimoto, K., Ogawa, S., Rane, J., Ishitani, M., Hara, N., Kitomi, Y., Inukai, Y., Ono, K., Kanno, N.*, et al.* (2013). Control of root system architecture by *DEEPER ROOTING 1* increases rice yield under drought conditions. Nat Genet *45*, 1097-1102.

Winter, D., Vinegar, B., Nahal, H., Ammar, R., Wilson, G. V., and Provart, N. J. (2007). An "Electronic Fluorescent Pictograph" Browser for Exploring and Analyzing Large-Scale Biological Data Sets. Plos One *2*.

Yamamoto, M., and Yamamoto, K. T. (1998). Differential Effects of 1-Naphthaleneacetic Acid, Indole-3-Acetic Acid and 2,4-Dichlorophenoxyacetic Acid on the Gravitropic Response of Roots in an Auxin-Resistant Mutant of Arabidopsis, *aux1*. Plant Cell Physiol *39*, 660-664.

1   **FIGURE LEGENDS**

2

3   **Figure 1. Natural variation of root growth responses upon NPA treatment.**

4   (**A**) Representative accessions of *A. thaliana* that show weak, intermediate, and strong

5   agravitropic growth on medium containing 10 μM NPA at 6 days after germination (DAG). Yellow

6   bars: 1 cm. (**B**) Distribution of phenotypes of NPA treated roots. Fold changes of trait values of

7   NPA treated accessions in comparison to untreated accessions were compared between two

8   traits (total length and horizontality, see supplementary information for details of traits.) x-axis:

9   trait; y-axis: fold change of traits under NPA treatment. (**C**) Quantile-quantile plot of *p*-values that

10   were calculated by GWAS. The line matching between x-y and x=y lines in the low *p*-value range

11   suggests no significant cofounding in GWAS. x-axis: expected *p*-values of SNPs; y-axis: observed

12   *p*-values of SNPs. (**D**) Manhattan plot for GWA mapping of the root angle phenotype. Manhattan

13   plot for the SNP associations to horizontality were obtained from GWAPP (Seren *et al.*, 2012).

14   Chromosomes are depicted in different colors. The horizontal dash-dot line corresponds to a

15   nominal 0.05 significance threshold after Bonferroni correction. Red box indicates the significantly

16   associated locus. See also Figure S1 and S2 and Table S1 and S2.

17

18   **Figure 2. *EXO70A3* expression levels and gene models in *EXO70A3*-related lines.**

19   (**A**) Gene models of *EXO70A3* mutants. Orange arrow: genomic sequence of coding region; Light

20   green boxes: exon; Gray bar: intergenic region; Green boxes: amino acid sequence; Lines

42

1 indicated by arrowheads and asterisks: points of mutation. See also Figure S2 and S3 and Table

2 S1 and S2. (**B**) Transcript levels of *EXO70A3* in different tissues of seven *A. thaliana* lines. x-axis:

3 sample; y-axis: relative expression level (normalized to Col-0 root tip); Error bars: standard

4 deviation; ND: not detected; Numbers above orange bars: fold change of *EXO70A3* transcript

5 level in each tissue of *35S::GFP:EXO70A3* in comparison with that in Col-0 root tip; "a", "b" and

6 "c": significance evaluated by ANOVA (p-value < 0.05, n = 3). (**C**) Transcript levels of *EXO70A3* in

7 different tissues of chemically treated Col-0 plants. x-axis: sample; y-axis: relative expression

8 level (normalized to mock-treated root tip); Error bars: standard deviation; ND: not detected.

9

10 **Figure 3. Natural *EXO70A3* variants determine high-response to NPA.**

11 (**A**) Root growth orientation response to NPA of Col-0 and *EXO70A3*-related mutant plants on

12 mock and 0.5 μM NPA media. x-axis: treatment; y-axis: angle changes of root tips at 1 day after

13 transfer (DAT) from 1 $\times$ MS plates to treatments medium at 5 DAG. (**B**) Beanplot showing root tip

14 angles of allelic complementation lines on mock and 0.1 μM NPA media. KO: *CRISR-exo70A3-1*;

15 AC: allelic complementation lines that were prepared by transforming *CRISR-exo70A3-1* with

16 vector control (AC$_{EV}$) or *EXO70A3* alleles from Col-0 (AC$_{Col-0}$), Shakdara (AC$_{Sha}$), Lp2-2 (AC$_{Lp2-2}$),

17 LAC-5 (AC$_{LAC-5}$) and Coc-1 (AC$_{Coc-1}$). Red characters indicate mutant-type alleles. x-axis:

18 treatments; haplogroup of alleles is indicated below x-axis; y-axis: angle changes of root tips at 1

19 DAT from 1 $\times$ MS plates at 5 DAG. Red lines: mean; short lines: individual data points; shape:

20 density of the data distribution; "a" and "b": significant difference evaluated by post hoc Tukey test

43

1   after ANOVA (*p*-value < 0.05, n ≥ 10). See also Figure S2.

2

3   **Figure 4. Perturbation of *EXO70A3* expression regulates PIN4 levels and patterns.**

4   Confocal images of representative roots of *PIN4::PIN4:GFP*, *DR5::GFP* or crosses with

5   *EXO70A3*-related lines grown on 1 × MS plates (5 DAG) and quantitative comparison of

6   fluorescent signal intensities. *PIN4:GFP* indicates *PIN4::PIN4:GFP*. Green: GFP signal; Red: cell

7   wall stained with propidium iodide (PI); White lines: outline of root tip; Yellow bars: 50 μm or 100

8   μm (indicated in each diagram). (**A**) Median longitudinal optical section of root tips (left panel), a

9   magnification of the left panel (second left panel) and maximum intensity projection (MIP) images

10 (three right panels) of *PIN4::PIN4-GFP*, *PIN4::PIN4-GFP CRISPR-exo70A3-1* and

11 *PIN4::PIN4-GFP EXO70A3ox*. (**B**) Quantitative comparison of GFP signal intensities among

12 *EXO70A3*-related mutants. x-axis: average relative signal intensity normalized by that in plants

13 with Col-0 background; y-axis: background line of crosses with *PIN4::PIN4:GFP* (left panels) or

14 DR5::GFP (right panels) that are tested in this diagram; Error bars: standard deviation; "a", "b" and

15 "c": significance evaluated by ANOVA (*p*-value < 0.05, n ≥ 10). (**C**) FRAP analysis of the EXO70A3

16 effects on cellular *PIN4::PIN4:GFP* transport. GFP signal in a columella cell was bleached after

17 three pre-scans and the recovery of signal intensity in the cell was measured. More than 10 cells

18 in different roots were analyzed per line. Signal intensities at all time points in all cells were

19 normalized by the average signal intensity of *PIN4::PIN4:GFP* cells of three pre-scans, and an

20 average value of each line was   plotted for each time point. x-axis: relative signal intensity;

44

1   y-axis: time (minute); Blue arrowheads: point of photo bleaching; T_{Half}: Half-time, a calculated time

2   which is necessary to obtain 50% of maximum recovery after photo bleaching, which is indicated

3   by a gray line for *PIN4::PIN4:GFP* and a magenta line for *PIN4::PIN4:GFP EXO70A3ox*; Error

4   bars: standard deviation. (**D**) Median longitudinal optical section of root tips (left panel) and

5   maximum intensity projection (MIP) images (two right panels) of *DR5::GFP*, *DR5::GFP*

6   *CRISPR-exo70A3-1* and *DR5::GFP EXO70A3ox*. (**E**) *DR5::GFP* signals at 3 hours after 90º turn.

7   White arrows: the gravity vector. Yellow arrowheads: optically visible ends of basipetally extended

8   GFP signals at the side of gravity vector under gravistimulation. See also Figure S3, S4 and S5.

9

10   **Figure 5. *EXO70A3* regulates rapidness of the gravitropic bending upon gravistimulus.**

11   (**A-F**) Re-orientation of root tips after 90º turning of plates measured in 32 minute intervals.

12   *CRISPR-exo70A3-1* (**A**), *CRISPR-exo70A3-2* (**B**), *EXO70A3ox* (**C**), *35S::GFP:EXO70A3* (**D**) and

13   *pin4-3* and *pin4-3 EXO70A3ox* (**E**) were compared with Col-0. In the same way, four natural

14   accessions from Haplogroup C and four natural accessions from Haplogroup H were compared

15   (**F**). x-axis: time [minutes] after plate turning; y-axis: average angle change of root tip; Error bars:

16   standard deviation; Beanplots: total root tip angle changes of Col-0 and *EXO70A3ox* after 6 or 10

17   hours; Red lines: mean; short lines: individual data points; shape: density of the data distribution;

18   Asterisks: significance evaluated by Welch t-test (p-value < 0.05, n $\geq$ 3) or significance evaluated

19   by population structure corrected association test for angle changes at 10h after re-orientation (**F**,

20   p-value < 0.05). See also Figure S3 and S5 and Movie S1 and S2.

1

Figure 6. *EXO70A3* alleles impact root system architecture.

Vertical-sections of representative root systems for various *EXO70A3*-related lines and natural

accessions grown in soil for 31 days. Red lines: traced roots from the image; Yellow bars: 10 cm.

(**A**) Representative images of original vertical-sections of a Col-0 plant. (**B**) Beanplot of the

horizontal/vertical expansion (Shallowness) of root systems (31 DAG) in Col-0, *CRISPR-exo70A3*,

EXO70A3ox, *pin4-3* and haplogroups C and H. x-axis: lines; y-axis: Shallowness; KO:

CRISPR-exo70A3-1; OX: *EXO70A3ox*; *pin*: *pin4-3*; C: haplogroup C accessions; H: haplogorup H

accessions; "a" and "b": significance evaluated by ANOVA (p-value < 0.05, n = 5) for Col-0 and

three mutant lines; Asterisk: significance evaluated by population structure-corrected association

test (*p*-value < 0.05, n = 4) for Haplogroup C vs. H. (**C**) Vertical-sections of representative root

systems for Col-0, *CRISPR-exo70A3-1*, *EXO70A3ox* and *pin4-3* (traced roots). (**D**)

Vertical-sections of representative root systems for haplogroup C and H accessions (traced roots).

See also Figure S7.

Figure 7. *EXO70A3* alleles associate with fitness in drought conditions.

(**A**, **B**) Beanplots showing distributions of the average seed numbers of Col-0, *EXO70A3ox*, and

haplogroups C and H in control (well-watered) (A) and drought conditions (B). x-axis: lines; y-axis:

average seed number of four plants grown in one pot (Col-0 and *EXO70A3ox*) or each accession

in four blocks of the experimental design (haplogroups C and H). Asterisk: significance evaluated

1   by ANOVA (p-value < 0.05); n.s.: not siginificant. (**C**) Reaction norms for seed numbers under

2   control (wet) and drought conditions. x-axis: treatment; y-axis: average seed numbers of Col-0

3   (magenta line), *EXO70A3ox* (cyan line), and haplogroups C (red lines) and H (blue lines). See

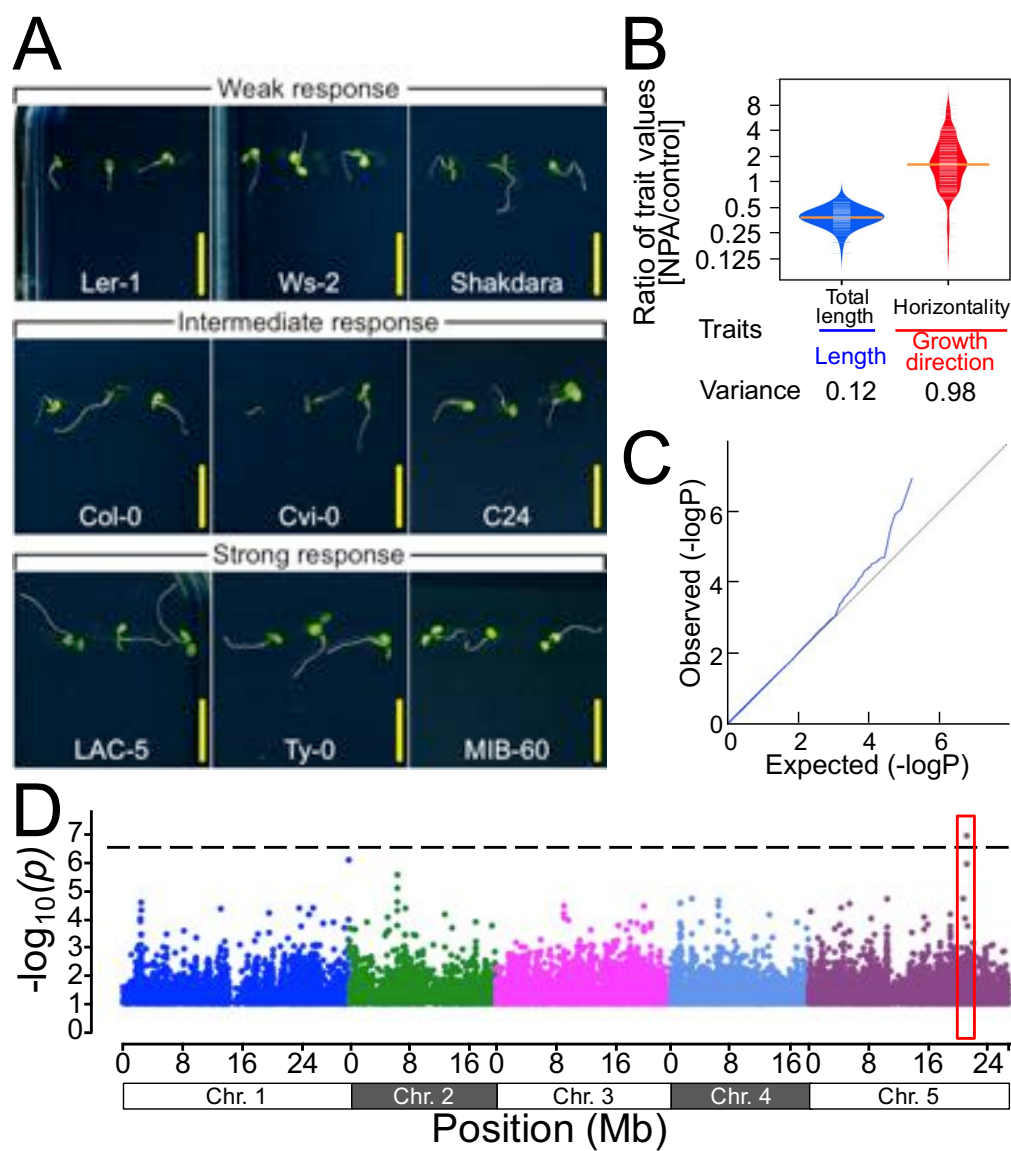4   also Figure S6 and S7 and Table S3.

5

A

Weak response
Ler-1 | Ws-2 | Shakdara

Intermediate response
Col-0 | Cvi-0 | C24

Strong response
LAC-5 | Ty-0 | MIB-60

B

Ratio of trait values [NPA/control]

Traits	Total length	Horizontality
	Length	Growth direction
Variance	0.12	0.98

C

Observed (-logP) vs Expected (-logP)

D

-log$_{10}$(p)

Position (Mb)

Chr. 1 | Chr. 2 | Chr. 3 | Chr. 4 | Chr. 5

Figure 1   Ogura et al. 2018

A

CRISPR-exo70A3-1: 3 bp deletion
CRISPR-exo70A3-2: 1 bp insertion

114 bp

971 bp

2708 bp

EXO70A3 Genomic

531 bp

T-DNA insertion (*EXO70A3ox*)

EXO70A3 CDS

1761 bp

587 residues

EXO70A3 Protein

CRISPR-exo70A3-1   114 R
CRISPR-exo70A3-2   47 R

Conserved EXOCYST domain

B

■ Col-0 □ *CRISPR-exo70A3-1* □ *CRISPR-exo70A3-2* ■ *pin4-3*
□ *EXO70A3ox* □ *35S::GFP:EXO70A3* □ *pin4-3 EXO70A3ox*

Relative expression level (fold change)

39971   40156   46771   21076   c

b   b

a   a

ND ND ND   ND   ND ND ND   ND   ND ND ND   ND   ND ND

Whole   Shoot   Root   Root tip

C

Relative expression level (fold change)

□ Mock
■ IAA
■ NPA

ND ND ND   ND ND ND   ND ND ND

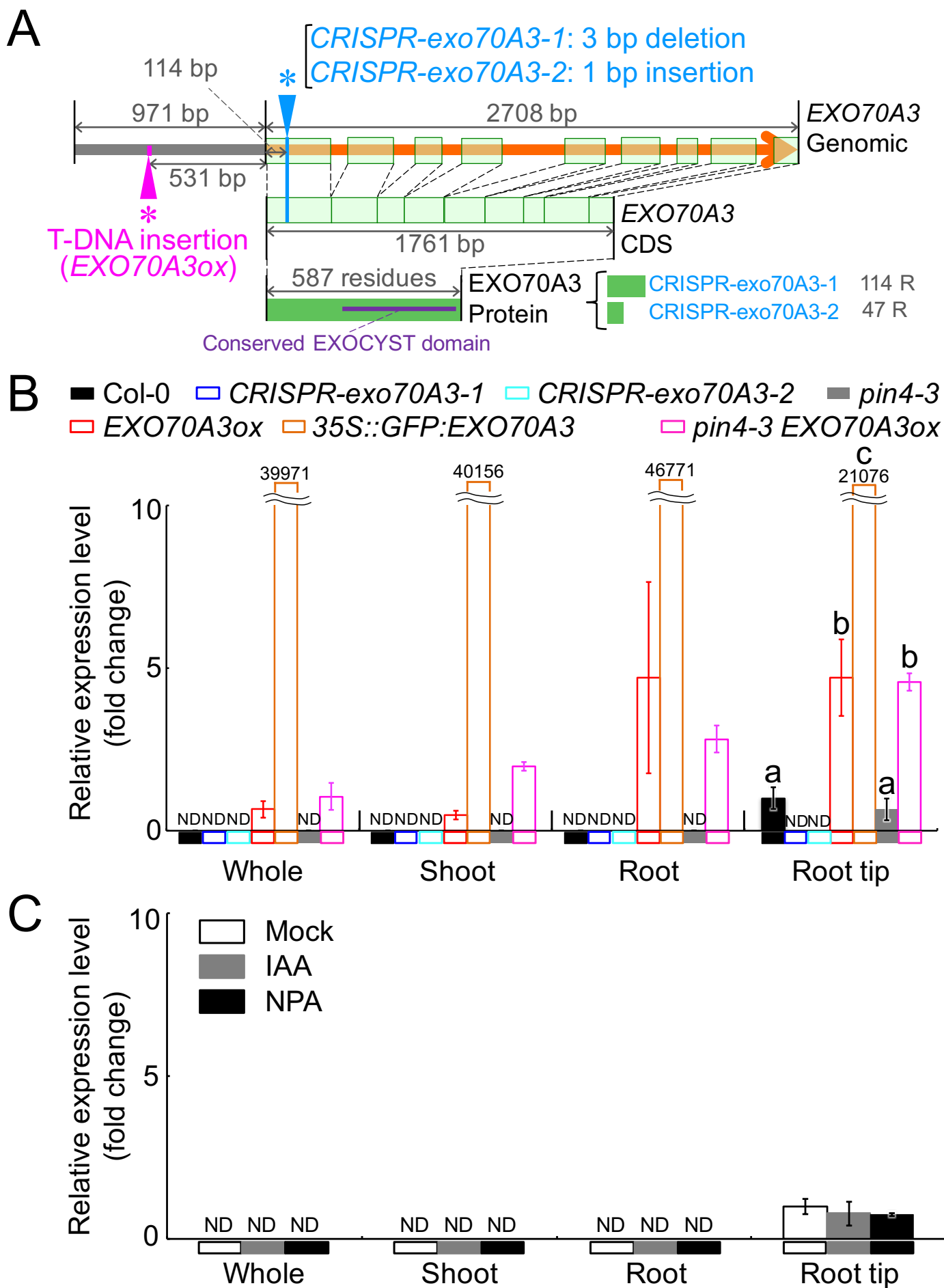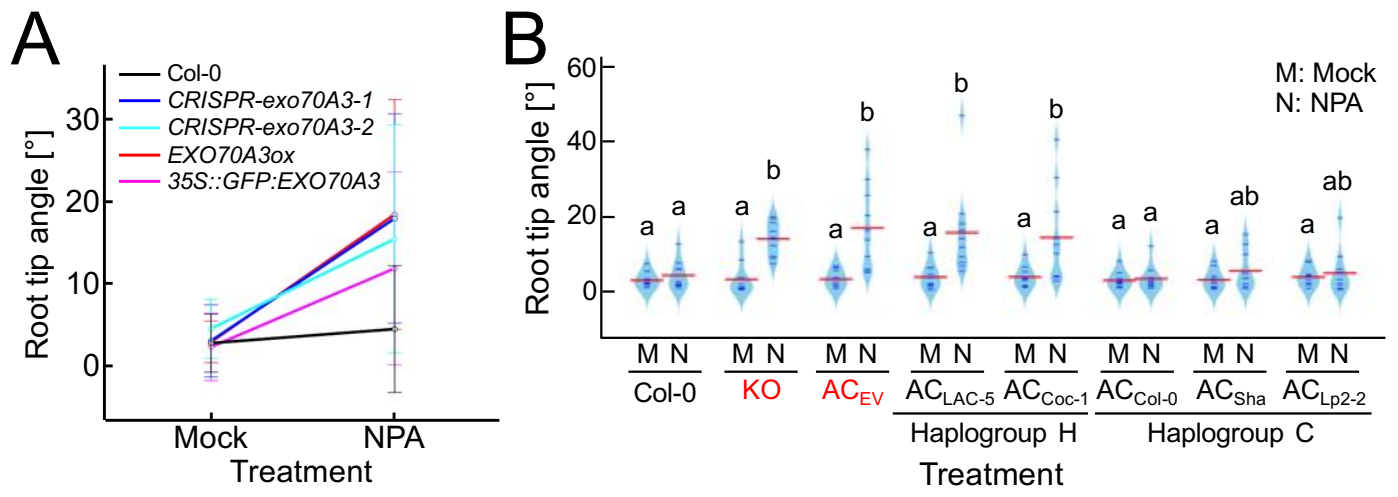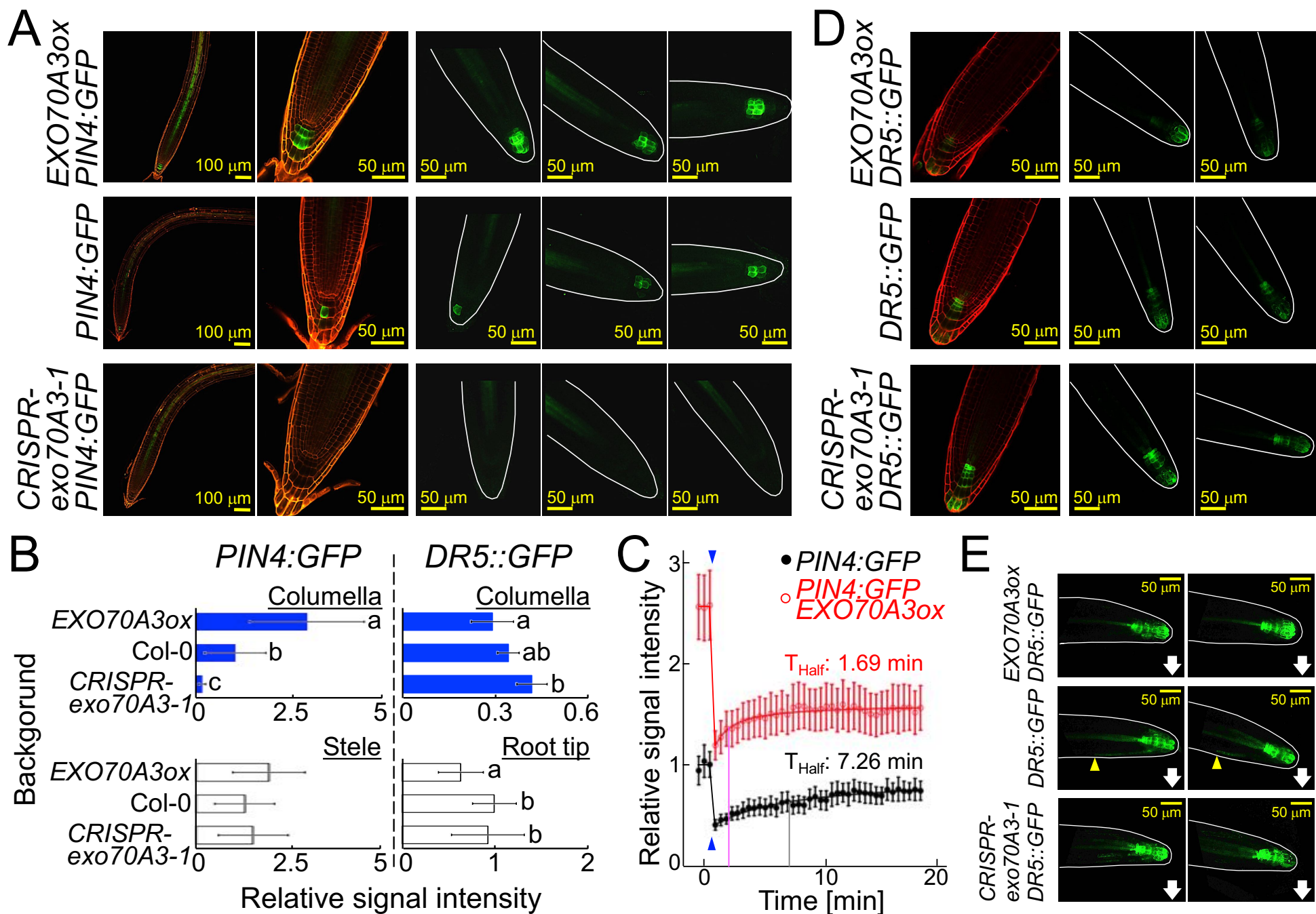Whole   Shoot   Root   Root tip

Figure 2   Ogura et al. 2018

Figure 3   Ogura et al. 2018

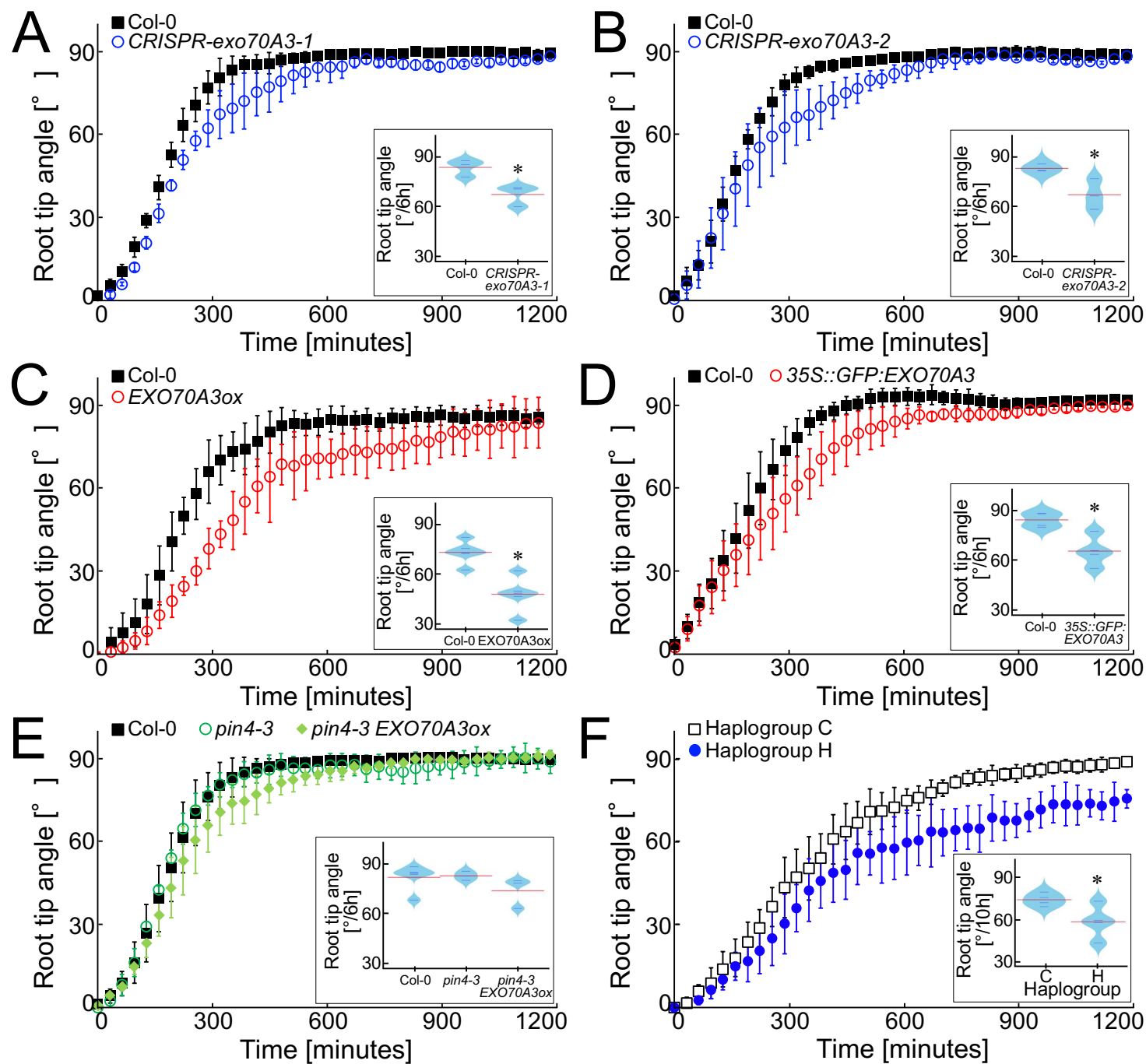Figure 4 Ogura et al. 2018
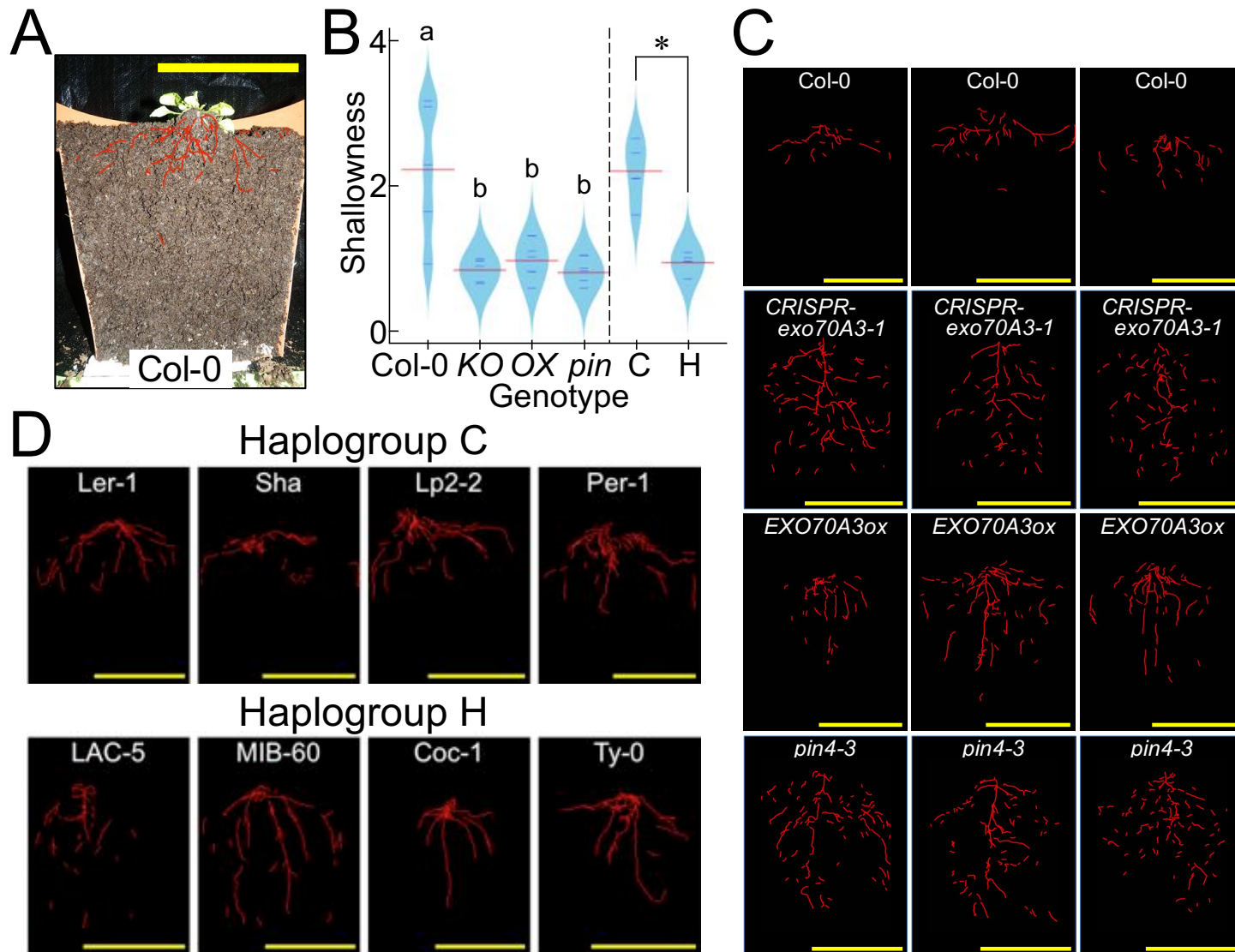
Figure 5   Ogura et al. 2018

A

Col-0

B

Shallowness vs Genotype (Col-0, KO, OX, pin, C, H)

C

Col-0 | Col-0 | Col-0
CRISPR-exo70A3-1 | CRISPR-exo70A3-1 | CRISPR-exo70A3-1
EXO70A3ox | EXO70A3ox | EXO70A3ox
pin4-3 | pin4-3 | pin4-3

D

Haplogroup C
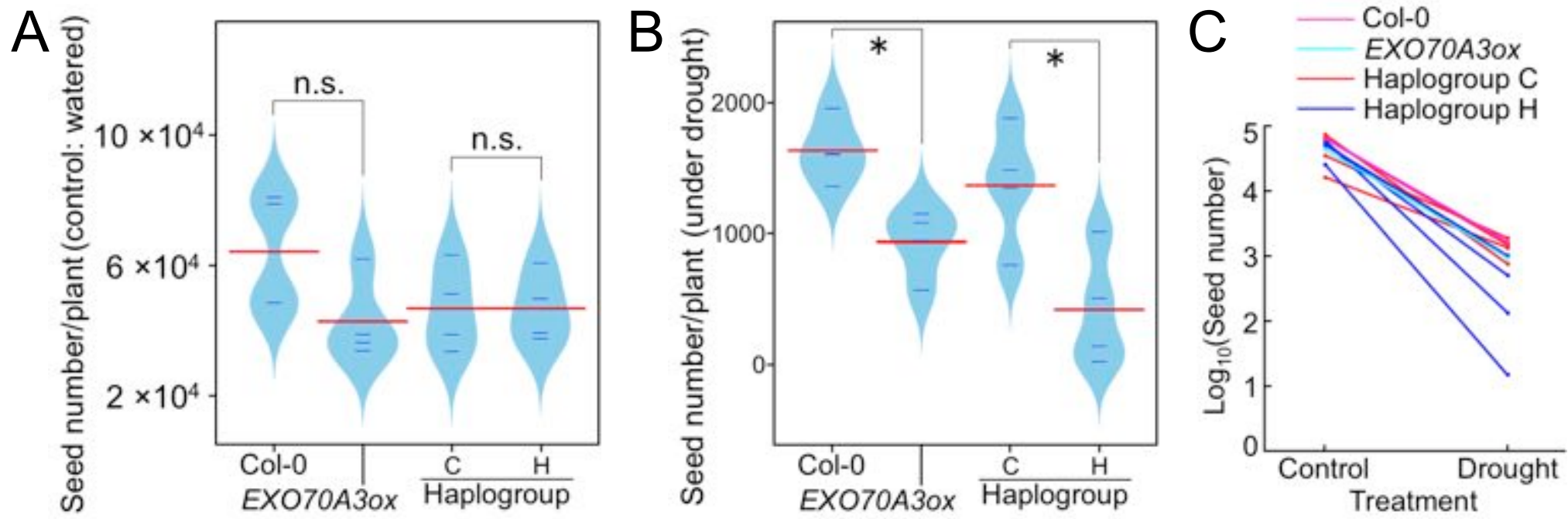
Ler-1 | Sha | Lp2-2 | Per-1

Haplogroup H

LAC-5 | MIB-60 | Coc-1 | Ty-0

Figure 6   Ogura et al. 2018

Figure 7   Ogura et al. 2018